European Review for Medical and Pharmacological Sciences 2022; 26: 148-157

The synergistic effect of palmitic acid and glucose on inducing endoplasmic reticulum stress-associated apoptosis in rat Schwann cells

D. YANG, J. XIE, X.-C. LIANG, Y.-Z. CUI, Q.-L. WU

Department of Traditional Chinese Medicine, Peking Union Medical College Hospital, Peking Union Medical College and Chinese Academy of Medical Sciences, Beijing, China

Dan Yang and Jun Xie contributed equally to this work

Abstract. – OBJECTIVE: Diabetic peripheral neuropathy (DPN) is a common long-term complication of diabetes mellitus accompanied with hyperglycemia and hyperlipidemia. Both high blood glucose and high blood lipids are key pathogenies for DPN. This research aims to investigate whether the combination of glucose (Glu) and palmitic acid (PA) played a synergistic role in the pathogenesis of DPN.

MATERIALS AND METHODS: The proliferation rate of Rat Schwann cell line RSC96 cells stimulated by different concentrations of Glu and PA were analyzed by CCK-8 assay. After the IC50 was detected for each drug, the RSC96 cells were divided into control, Glu, Glu+PA, PA, and BSA groups. The apoptosis of RSC96 cells in different groups were detected by flow cytometry. The effects of Glu and/or PA on endoplasmic reticulum (ER) stress-associated apoptotic signaling pathways were determined by Western blot and qPCR.

RESULTS: Both Glu and PA showed similar inhibition on the proliferation of RSC96 cells in a dose-dependent manner. However, PA induced stronger apoptosis of RSC96 cells than glucose and significantly increased the levels of X-box-binding protein-1 (XBP1), C/EBP homologous protein (CHOP), and eIF2α phosphorylation, which are key proteins regulating endoplasmic reticulum (ER) stress-associated apoptotic signaling pathways. The combination of Glu and PA induced the strongest apoptosis in RSC96 cells and also activated ER stress-associated apoptotic signaling pathways. These results verified the synergistic effect of Glu and PA on inducing ER stress-associated apoptosis in RSC96 cells, and PA even induced stronger apoptosis in RSC96 cells than Glu.

CONCLUSIONS: The present research indicated that hyperglycemia and hyperlipidemia might exert a synergistic damage during the pathogenesis of DPN, suggesting that blood lipid control is as important as blood glucose control for DPN patients.

Key Words:
Diabetes mellitus, Palmitic acid, Glucose, Endoplasmic reticulum stress, Apoptosis, Schwann cells.

Introduction

Diabetes mellitus is becoming a global health issue. It is estimated that the prevalence of diabetes mellitus will reach 642 million by 2040[1,2]. Diabetic patients usually accompany with a range of microvascular complications (e.g., retinopathy, nephropathy, and peripheral neuropathy), and macrovascular complications (e.g., peripheral vascular disease and ischemic heart disease)[3,4]. Diabetic peripheral neuropathy (DPN) is a common complication of diabetes mellitus with high morbidity rate and mortality rate, and reduced living quality[5-7]. Schwann cell (SC) is the primary glia cell of the peripheral nervous system, which plays crucial roles in peripheral nervous system. It is not only involved in the development and regeneration of neurons, but also provides the trophic support for neurons[8,9]. Consistent exposure to extreme high levels of glucose leads to SC deficiency, which contributes to DPN[9,10].

Currently, high levels of blood glucose are considered as a major cause of diabetic complications, including angiopathy and neuropathy. However, the theory of hyperglycemia as the prevalent cause of diabetic complications was challenged by researchers. There were about 40% of diabetic patients who still developed neuropathy even though their blood glucose levels were well controlled. Pitenger et al[11] reported that serum from Type 1 diabetic patients showed toxic effect on neurons independent of serum glucose levels. Thus, there might be some components in the serum of diabetic pa-

Corresponding Author: Qunli Wu, MD; e-mail: weiyi123@163.com

tients rather than glucose which cause damage to peripheral nerves, leading to DPN.

Patient's metabolic status also contributes to the pathogenesis of neuropathy, such as obesity and hyperlipidemia[4,12]. In a cohort of participants with mild to moderate diabetic neuropathy, elevated triglycerides are correlated with the loss of sural nerve myelinated fiber density, which is independent of blood glucose level, disease duration, age, and other variables. These data suggest that hyperlipidemia is correlated with the progression of diabetic neuropathy[13]. The levels of serum monounsaturated free fatty acid (FFA) oleic acid (OA, 18:1) and the saturated FFA palmitic acid (PA, 16:0) are always increased in obese and type II diabetic patients[14].

The overloaded lipid in non-adipose tissues can cause cell deficiency and cell death, which is known as lipotoxicity. The consistent exposures of non-nerve cells to high levels of FFA result in lipotoxicity[15-17]. Elevated levels of FFAs in diabetic and obese individuals promote TNF-alpha-mediated cell death of vascular smooth muscle cells[16]. The quick accumulation of FFAs in certain pathophysiological conditions, such as brain or spinal cord damages, could contribute to the death of nerve cells[18,19]. *In vitro* exposure of myenteric neuron to high levels of PA leads to neuronal shrinkage and reduced neuronal survival rate[14]. These reports suggest that FFA overload plays a critical role in cell death of neurons.

Recent reports[20-22] emphasize the role of endoplasmic reticulum (ER) stress in the development of DPN. ER stress is a cellular process, triggered by the accumulation of abnormal folding proteins in the ER lumen. ER stress stimulates the unfolded protein response (UPR), aiming to remove unfolded or misfolded proteins and to restore ER homeostasis. Failure recovery from the ER stress usually leads to cell death[23,24]. Salubrinal treatment, a specific inhibitor of eukaryotic initiation factor-2alpha (eIF-2α) dephosphorylation, suppressed ER stress in a high-fat diet fed mouse model with impaired glucose tolerance, leading to the alleviation of peripheral nerve dysfunction[22]. In a streptozotocin-induced diabetic mouse model with C/EBP homologous protein (CHOP) deficiency, trimethyloxide therapy enhanced expression of folding protein-glucose-regulated protein 78 (GRP78) and improved peripheral nerve function, compared to wild-type mice[25]. These findings suggest an important role of ER-stress in the development of DPN.

In this study, we investigated the interaction between elevated levels of glucose (Glu) and PA in the development of diabetic neuropathy. We treated SC with different concentrations Glu and/or PA for different time durations, and found that PA played a dominant role in cell death of SC. The combination of Glu and PA showed a synergistic damage to SC. Moreover, both PA and the combination treatments activated multiple ER stress signal pathways. These data indicated that pathological conditions with lipid elevation might cause ER stress and SC dysfunction. The combination of high blood glucose and blood lipid synergistically activated the ER stress-associated apoptosis signal pathways. Our findings verified the important role of Glu and PA in DPN associated with the induction of ER stress, which provided a potential new therapeutic target for DPN.

Materials and Methods

Cell Lines and Culture Condition

The Rat Schwann cell line RSC96 was obtained from China Center for Type Culture Collection (CCTCC). RSC96 cells were maintained in common Dulbecco's Modified Eagle's Medium (DMEM; Gibco, Rockville, MD, USA) supplemented with 10% fetal bovine serum (FBS; Gibco, Rockville, MD, USA) and 100 U/mL penicillin-streptomycin (Gibco, Rockville, MD, USA), and grown at 37°C in a humidified atmosphere containing 5% CO_2.

Cell Viability Assay

RSC96 cells were seeded onto a 96-well plate with 2×10^3 cells/well at logarithmic phase. Additional Glu was dissolved in 1×phosphate buffered saline (PBS) and PA solution was prepared with 0.4% bovine serum albumin (BSA) in 1×PBS. After 24 h, the medium was replaced with fresh completed DMEM medium containing different concentrations of Glu (25, 50, 100, 200, 300 mM), PA (0.2, 0.4, 0.6, 0.9 mM; Gibco, Rockville, MD, USA). The same volume of 300 mM mannose (Sigma, St. Louis, MO, USA) was added into the control group to keep a similar osmotic potential, and 0.4% BSA (Sigma, St. Louis, MO, USA) was added into the vehicle control group. Five parallel duplicate wells were set under each condition. The treatments were maintained for 24 h separately, and cell proliferation was determined by Cell Counting Kit-8 (CCK-8) according to the manufacturer's instructions (Beyotime, Shanghai, China). Briefly, 10 μL of CCK-8 solution was added to each well and cells were further incubated at 37°C for 3 h. The absorbance value (OD_{450}

value) was measured at a wavelength of 450 nm with an automatic microplate reader.

Grouping

RSC96 cells were randomly divided into control group and four groups with different treatments: Glu group (100 mM Glu), Glu+PA group (100 mM Glu and 0.4 mM PA/BSA), PA group (0.4 mM PA/BSA), or BSA group (0.4% BSA). In the control group, the same volume of 100 mM mannose was added to culture medium to keep a similar osmotic potential compared to other treatment groups. Five parallel duplicate wells were set under each condition. Cells were incubated at 37°C for 12 h, 24 h, or 48 h separately. Cell viability was detected by CCK-8 assay, and cell morphology was recorded under an inverted microscope.

Flow Cytometric Apoptosis Assay

Cell apoptosis was analyzed by using an Annexin V-FITC Apoptosis Assay kit according to the manufacturer's instructions (Beyotime, Shanghai, China). Briefly, cells were resuspended in the binding buffer, and then, stained with 5 μL of annexin V-FITC and 10 μL of propidium iodide (PI). The cells were incubated for 20 min in the dark under room temperature. Cells were then analyzed using a Gallios flow cytometer (Beckman, Franklin Lakes, NJ, USA). Data were analyzed with Kaluza software (version 1.3). The quadrant was draw according to the outlines of PI^-Annexin V^- and PI^+Annexin V^+ cell populations.

Western Blotting

Stimulated cells were harvested and dissociated in RIPA lysis buffer (Beyotime, Shanghai, China) containing protease inhibitor (Complete, Roche, Basel, Switzerland). All the selected protein extracts of each group cells were resolved by 12% SDS-PAGE and transferred on polyvinylidene difluoride (PVDF) membranes (Millipore, Billerica, MA, USA). PVDF membranes were blocked with 5% skim milk (Yuanye, Shanghai, China) for 1 h at room temperature and incubated overnight with GRP78 antibody (1:1000, Cell Signaling, Danvers, MA, USA, Cat#: 3183s), XBP1 (0.3 μg/mL, BioLegend, San Diego, CA, USA, Cat#: 619502), CHOP (0.4 μg/mL, Santa Cruz, Santa Cruz, CA, USA, Cat#: sc-7351), eIF-2α (2 μg/mL, MultiSciences Biotech, Hangzhou, China, Cat#: ab32795), Phospho-eIF-2α (2 μg/mL, MultiSciences Biotech, Hangzhou, China, Cat#: ab30251), Cleaved caspase-3 (1:1000, Cell Signaling, Danvers, MA, USA, Cat#: 9664s), β-actin (0.5 μg/ mL, MultiSciences Biotech, Hangzhou, China, Cat#: ab008), or GAPDH (0.5 μg/mL, MultiSciences Biotech, Hangzhou, China, Cat#: Mab5465) at 4°C. The secondary antibody conjugated with HRP (1:5000, Lianke, Hangzhou, China) was incubated for 2 h at room temperature. Signals were detected using an HRP Enhanced Chemiluminescent Kit (BI) and images were scanned.

Quantitative Real-Time PCR (qRT-PCR)

RNA from RSC96 cells was separated by RNeasy Mini kit (Qiagen, Hilden, Germany), and complementary deoxyribose nucleic acid (cDNA) was synthesized by a RevertAid First Strand cDNA Synthesis Kit (Thermo Scientific, Waltham, MA, USA). Gene expression of spliced XBP1 was determined by real-time PCR with Thermo SYBR green/ROX (Thermo Scientific, Waltham, MA, USA) and primers (sXBP1-For: GCAGCAAGTGGTGGATTTGG, sXBP1-Rev: CACCTGCTGCGGACTCA) in a 7500 Real-Time PCR system (Applied Biosystems, Foster City, CA, USA). The fold changes of gene expression were analyzed by using the comparative threshold cycle method and normalizing to rat β-actin as the reference gene (β-actin-For: ACCCGCGAGTACAACCTTCTT, β-actin-Rev: GACCCATACCCACCATCACAC). The specificity of the PCR products was determined by dissociation curves.

Statistical Analysis

Data were expressed as means ± SEM (Standard Error of Mean) and analyzed using Prism software (version 7, GraphPad, La Jolla, CA, USA). Student's *t*-test (unpaired, two sided) was used for comparing two groups. One-way analysis of variance (ANOVA) with Tukey's post-hoc test was used for multi-group comparisons. Values were considered statistically significant when $p<0.05$. Significant differences and the *p*-values are represented in figures by asterisks as follows: * $p<0.05$; ** $p<0.01$; *** $p<0.001$.

Results

High Levels of Glu and PA Inhibited Schwann Cell Proliferation in a Dose-Dependent Manner

As shown in Figure 1A, Glu showed dose-dependent inhibition on cell proliferation of SC. The OD_{450} value reduced more than 50% compared to control (300 mM mannose), when the concentration of Glu was above 200 mM. The IC50 for

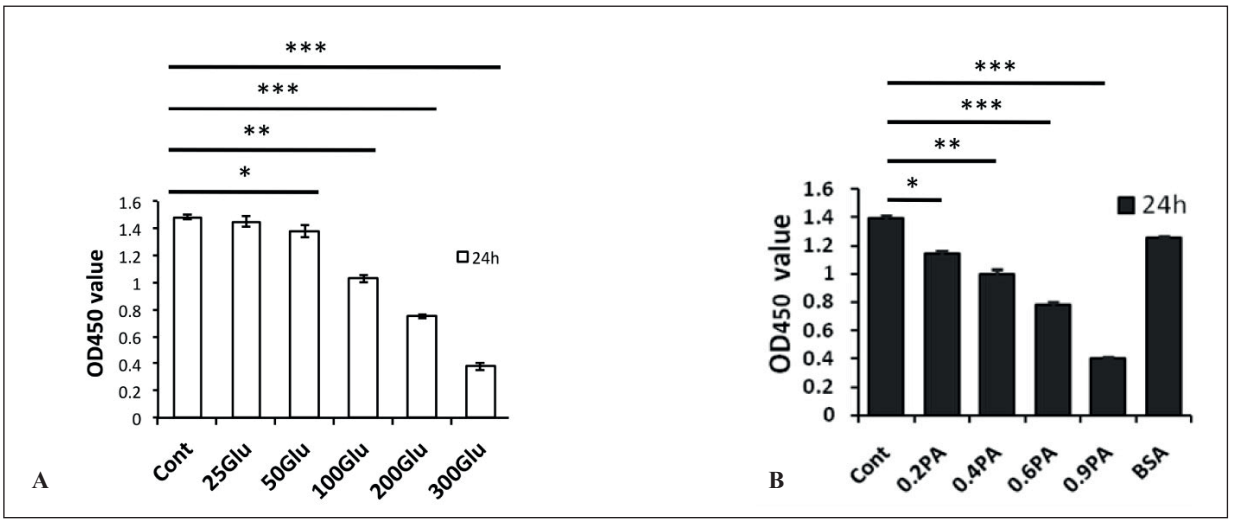

Figure 1. High concentrations of glucose (Glu) and palmitic acid (PA) inhibit Schwann cell proliferation in a dose-dependent manner. RSC96 cells (SC) were seeded onto a 96-well plate with 2×10^3 cells/well. After 24 h, the cultures were treated with increasing concentrations of Glu (25, 50, 100, 200, 300 mM) or PA (0.2, 0.4, 0.6, 0.9 mM). The same volume of 300 mM mannose or 0.4% BSA was added into the control and vehicle control group, respectively. Cell proliferation was determined in the indicated time duration by using a Cell Counting Kit-8 (CCK-8) according to the manufacturer's instructions. Glu inhibited SC proliferation in a dose-dependent manner at 24 h (**A**). PA inhibited SC proliferation in a dose-dependent manner at 24 h (**B**). Five parallel duplicate wells were set under each condition and the experiments were repeated four times. Data are mean ± SEM (Standard error of mean), and one-way ANOVA was used for statistical analysis. * $p<0.05$, ** $p<0.01$, *** $p<0.001$ versus control.

Glu is 100 mM. As shown in Figure 1B, all the tested concentrations (0.2-0.9 mM) of PA showed significantly inhibition on SC proliferation in a dose-dependent manner. The OD_{450} value reduced more than 50% compared to control group, when the concentration of PA was above 0.6 mM (Figure 1B). The IC50 for PA is 0.4 mM.

The Combination of Glu and PA Inhibited Schwann Cell Proliferation in a Synergistic Way

As shown in Figure 2, Glu (100 mM) and PA (0.4 mM) showed similar suppression on SC proliferation at different time points, compared to the control group (100 mM mannose). The com-

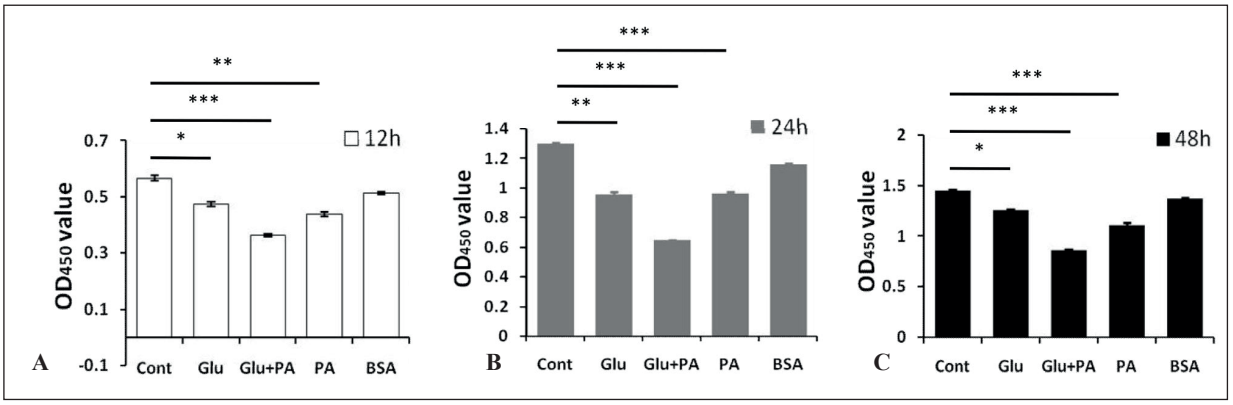

Figure 2. The combination of Glu and PA inhibited Schwann cell proliferation in a synergistic way. The combination of PA (0.4 mM) and Glu (100 mM) showed synergistic inhibition on SC proliferation, compared to control (100 mM mannose) at 12 h (**A**), 24 h (**B**), and 48 h (**C**) separately. Five parallel duplicate wells were set under each condition and the experiments were repeated four times. Data are mean ± SEM (Standard error of mean), and one-way ANOVA was used for statistical analysis. * $p<0.05$, ** $p<0.01$, *** $p<0.001$ versus control.

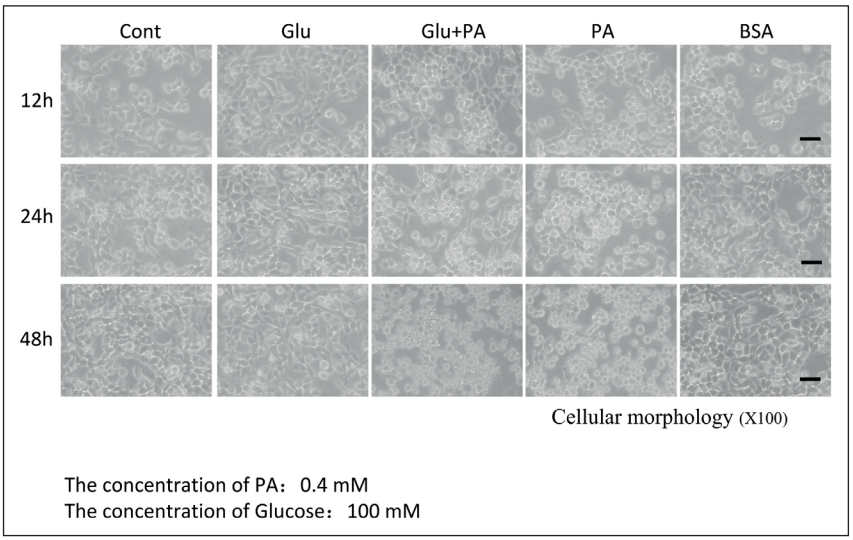

Figure 3. The combination of Glu and PA significantly affect the morphology of Schwann cells. SCs were cultured for 24 hours and then treated with PA (0.4 mM), Glu (100 mM) or their combination. Cell morphology was recorded at 12 h, 24 h or 48 h post-treatments under inverted microscope. The experiments were repeated three times independently (magnification, ×100. Scale bars, 100 μm).

bination of Glu and PA showed greater inhibition compared to single Glu or PA treatment at different time points. The greatest inhibition time point was observed at 24 h. No difference was observed between vehicle group (0.4% BSA) and control group at different time points.

As shown in Figure 3, After 24-hour or 48-hour treatment, the majority of cells in Glu+PA or PA groups became shrunk, rounded and floating, compared to control group, while cells in Glu group became long and thin without other changes. These results might suggest that PA and the combination of Glu and PA treatment caused more severe morphology change than Glu alone. Therefore, these data illustrated that high concentrations of either Glu or PA inhibited SC proliferation significantly, and the combination treatment showed a synergistic effect.

The Combination of Glu and PA Induced Schwann Cell Apoptosis in a Synergistic Way

Cell apoptosis was determined by analyzing the translocation of phosphatidylserine (PS) by Annexin V-FITC and cell death by PI. After 24-hour treatment, the percentages of the late apoptosis events (Annexin-V^+PI^+ cells) were significantly increased in Glu+PA group and PA group, compared to both Glu group and control group (Figure 3A). After 48-hour, Glu+PA and PA treatments not only further increased the percentages of the late apoptosis events (44.5% and 29.33%, respectively), but also elevated the proportions of the early apoptosis events, compared to control and Glu groups (Figure 3B, 3C). However, Glu treatment only increased the percentages of late apoptosis at 48 h, compared to control group (Figure 3C). Furthermore, Glu+PA group induced the largest percentage of apoptosis among all the groups in both early and late apoptosis (Figure 4). Thus, all these data suggested that PA induced stronger apoptosis than Glu in Schwann cells, and the combination of them exerted a synergistic effect in inducing SC apoptosis.

The Combination of PA and Glu Induced Endoplasmic Reticulum Stress-Associated Apoptosis Synergistically

ER-stress related proteins including GRP78, X-box binding protein 1 (XBP1), eIF-2α, and CHOP were analyzed by Western blot. As shown in Figure 5A, GRP78 protein expression level was increased after 24-hour treatments of Glu, PA or Glu+PA, compared to control group. The protein levels of XBP1 and CHOP, as well as spliced *Xbp1* gene expression level, were significantly increased in PA or Glu+PA group after 24-hour treatment, compared to both control and Glu groups (Figure 5A and Figure 6). After 48-hour treatment, the effects of Glu on GRP78 were disappeared, while the protein levels of XBP1 and CHOP remained increasing in PA and Glu+PA groups, compared to control and Glu groups (Figure 5B). Furthermore, PA or Glu+PA treatments also increased the phosphorylation of eIF-2α, compared to control and Glu groups (Figure 5C), indicating that PA might activate eIF-2α signaling pathway. The cleavage of caspase 3 was also analyzed, as a frequently ac-

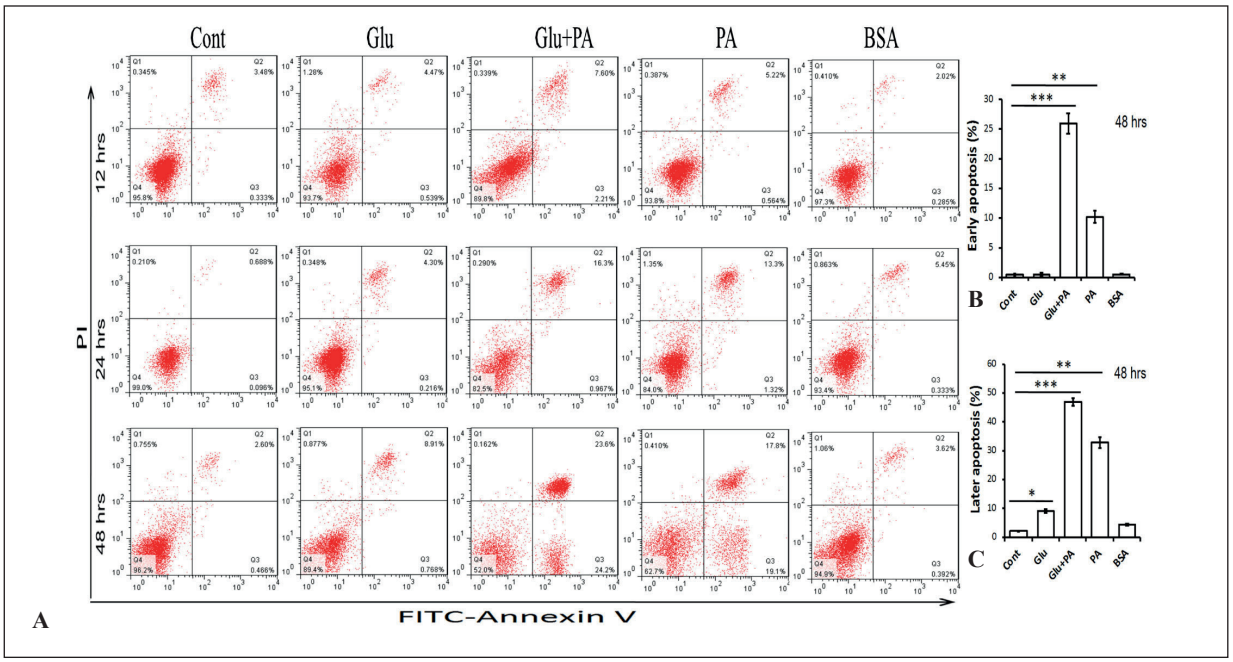

Figure 4. The combination of Glu and PA induced Schwann cell apoptosis in a synergistic way. SCs were cultured for 24 hours and then treated with PA (0.4 mM), Glu (100 mM) or their combination. Cells were harvested at 12 h, 24 h, and 48 h post-treatment for apoptosis analysis by using an Annexin V-FITC Apoptosis Assay kit according to the manufacturer's instructions. Annexin V-FITC$^+$PI$^-$ cell population is at the early stage of apoptosis, and Annexin V-FITC$^+$PI$^+$ cell population is at the late stage of apoptosis. Representative flow cytometry figures showed SC apoptosis (**A**). Statistical analysis of early (**B**) and late (**C**) stages of SC apoptosis at 48 h after treatments. The experiments were repeated three times with similar data. Data are mean ± SEM, and one-way ANOVA was used for statistical analysis. * p<0.05, ** p<0.01, *** p<0.001 versus control.

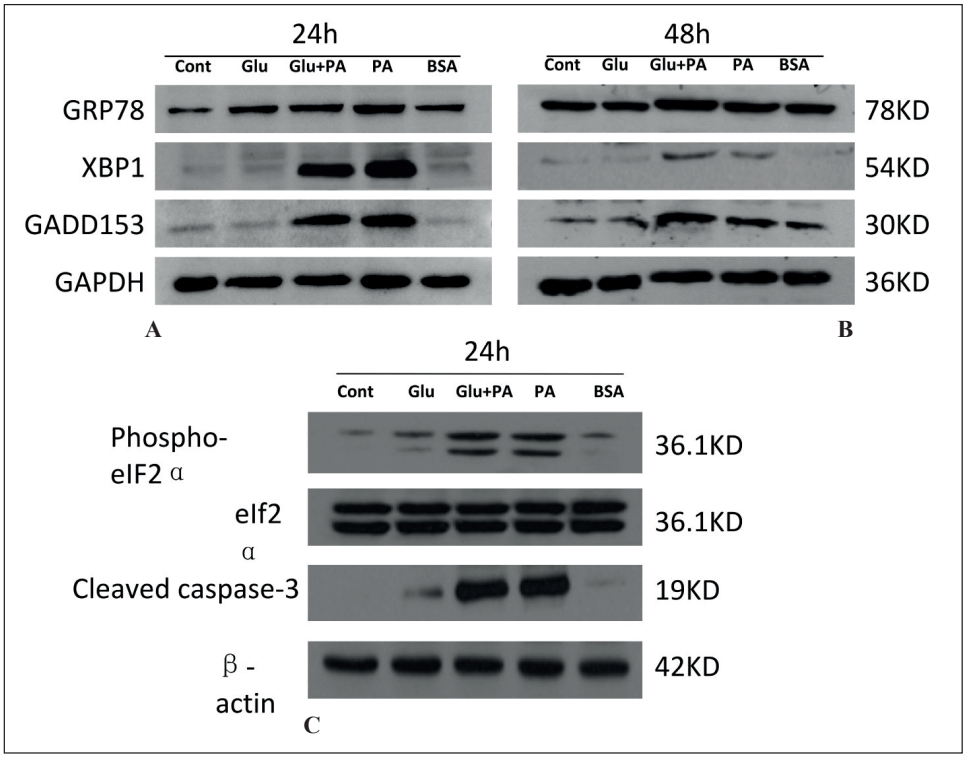

Figure 5. The combination of Glu and PA treatment induces ER stress-associated apoptosis in Schwann cells synergistically. Protein levels of GRP78, XBP1, CHOP, eIF-2α, eIF-2α phosphorylation, Caspase 3 cleavage, GAPDH, and β-actin of in different groups at 24 h (**A, C**) and 48 h (**B**). The experiments were repeated three times independently.

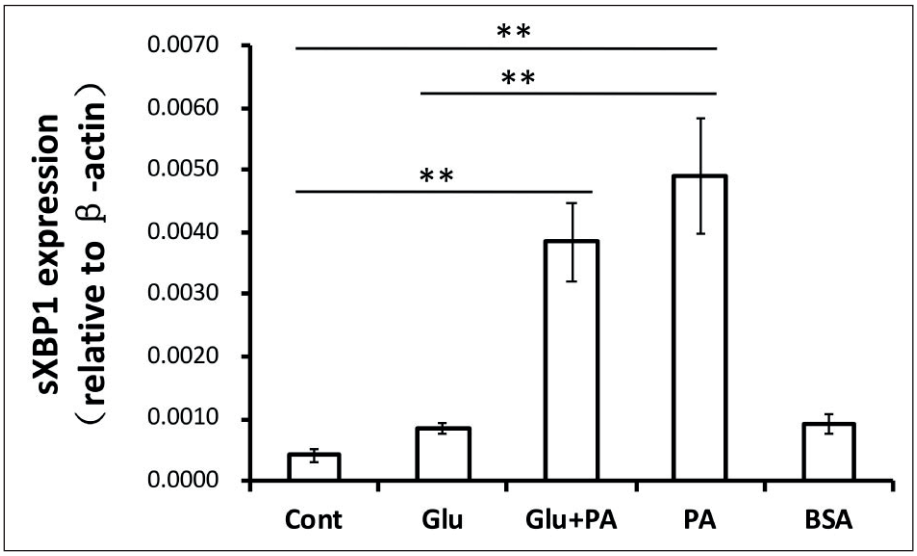

Figure 6. mRNA Levels of spliced XBP1 (sXBP1) of Schwann cells in different groups. Schwann cells were harvested for total RNA extraction and cDNA synthesis. qPCR was used to determine the mRNA Levels of spliced XBP1 (sXBP1) of Schwann cells in different groups. The experiments were repeated three times with similar results. Data are mean ± SEM, and one-way ANOVA was used for statistical analysis. ** $p<0.01$ versus control.

tivated death protease in cell apoptosis associated with ER stress. Consistent to the significant impacts of PA on SC apoptosis (Figure 3), both PA group and Glu+PA group induced the cleavage of caspase 3, compared to control and Glu groups (Figure 5C). Together, these data suggested Glu-combined with PA induced endoplasmic reticulum stress-associated apoptosis signal pathways synergistically.

Discussion

Diabetes mellitus is a chronic metabolic disorder. Long-term complications, such as retinopathy, nephropathy, and neuropathy, are major causes of the high morbidity, mortality and reduced quality of life[26-28]. Among them, DPN affects more than 50% of diabetic patients. High levels of blood glucose have long been considered as a major cause of diabetic-associated complications[29-32]. In this study, we found that high levels of either glucose or PA significantly inhibited proliferation of SC. However, high levels of PA showed a stronger inhibition on the RSC96 cells viability, and induced stronger apoptosis compared to high concentration of glucose. Furthermore, the combination of Glu and PA showed a synergetic effect on the inhibition of cell proliferation and induction of apoptosis. The Western blot results showed that both PA and Glu+PA groups upregulated the expression of GRP78, XBP1, CHOP, and the phosphorylation of eIF-2α in SC, while Glu group only slightly affected GRP78 expression. Together, these data suggested the synergistic effect of Glu and PA on inducing endoplasmic reticulum stress-associated apoptosis in RSC96 cells, and emphasized the importance of consistent lipid over-exposure during the pathogenesis of DPN, as well as hyperglycemia.

To characterize the effects of high concentrations of PA and Glu on the peripheral nerve system, Schwann cell is commonly used for *in vitro* study. RSC96 cell lines is spontaneously transformed Schwann cell lines derived from long-term culturing primary Schwann cells[33-35] with stable functional and pathophysiological characters, which is widely used in neuroscience researches.

ER stress is a critical process leading to cell death, which is usually due to the accumulation of unfolded proteins in the lumen of the ER followed with the activation of ER stress-associated signaling pathways[23,36]. ER stress response is an adaptive process and highly regulated by at least three signaling pathways[37,38]. The first response is to reduce the synthesis of new protein and to prevent the further accumulation of unfolded proteins[39]. The second response is to increase expression of chaperone proteins, such as GRP78, and to enhance the protein-folding capacity[40,41]. The third response is to eliminate damaged cells *via* the induction of apoptosis, which occurs when the ER is severely damaged[42]. Upon ER stress, the phosphorylation of IRE1 promotes the splicing of XBP1 mRNA. Spliced Xbp1 could induce ER-associated degradation chaperones, e.g., GRP78[43-45]. The upregulation of GRP78 is frequently correlat-

ed with cell survival[46,47]. In addition, spliced Xbp1 can also activate the transcription of CHOP (also known as GADD153)[48,49]. CHOP is a major signal pathway that promotes ER stress-associated cell death[43,50,51]. Therefore, XBP1 is able to simultaneously regulate the pro-survival and pro-apoptosis signaling pathways.

Interestingly, we found that PA or Glu+PA dramatically upregulated expression of XBP1, GRP78, and CHOP at both 24 and 48 h. However, the increased folds of CHOP compared to control were much higher than that of GRP78. This is consistent with the flow cytometry results, showing that PA or Glu+PA significantly induced SC apoptosis, compared to control and glucose groups.

Consistent with previous reports[52-58], our results verified that high levels of glucose inhibited SC proliferation and induced apoptosis. However, it did not significantly affect ER stress-related signaling pathways, indicating that high levels of glucose and PA may suppress SC proliferation *via* distinct mechanisms. Accumulating research evidences suggest that hyperglycemia causes glucotoxicity *via* several mechanisms, including the activation of poly-ADP-ribose polymerase and the induction of oxidative stress[54-57].

Although hyperglycemia is the most common characteristic of diabetic patients, hyperlipidemia, obesity, and hypertension are frequently observed in diabetic patients as well. More and more attention has been paid to the interplay between hyperglycemia and hyperlipidemia in DPN. Our study suggested that both hyperglycemia and hyperlipidemia suppressed SC proliferation, and the combination of them synergistically induced SC apoptosis, indicating that blood lipid control is as important as blood glucose control for DPN patients.

We firstly verified the synergistic effect of PA and glucose in the pangenesis of DPN, which was mediated by ER stress-associated signal pathway. In this study, we found that PA and glucose not only inhibited SC proliferation but also induced SC apoptosis. To our surprise, their combination showed stronger impacts on both the proliferation and apoptosis of SC, compared to either of them. Consistent to their synergistic effects, the combination of glucose and PA induced endoplasmic reticulum stress-associated apoptosis signal pathways in SC synergistically. These findings highlight the differential impacts of hyperglycemia and hyperlipidemia in DPN, and their synergistic effect in the pathogenesis of DPN. It emphasized the pathogenic role of PA and the combination of Glu and PA in DPN associated with ER stress, which provided a potential new therapeutic target for DPN.

Conclusions

Our study illustrated the synergistic effect of PA and Glu on inhibiting proliferation and inducing ER stress-associated apoptosis in Rat Schwann cells. Both high concentration of PA and Glu suppressed SC proliferation in a dose-depended manner. However, the combination of PA and Glu inhibited cell viability and induced ER stress-associated apoptosis in RSC 96 cells more significantly than single PA or Glu. These findings highlight the synergistic effect of hyperglycemia and hyperlipidemia in the pathogenesis of DPN, indicating that blood lipid control is as important as blood glucose for DPN patients.

Conflict of Interests

The authors declare that they have no known competing financial interests or personal relationships that could have appeared to influence the work reported in this paper.

Acknowledgments

This work was supported by the Natural Science Foundation of Beijing Municipality (Beijing Natural Science Foundation, No. 7152122, to QW).

Funding Acknowledgements

General Project of Beijing Natural Science Foundation (7152122); Beijing Dongcheng District Outstanding Talent Funding Project (2019DCT-M-09).

References

1) L'Heveder R, Nolan T. International diabetes federation. Diabetes Res Clin Pract 2013; 101: 349-351.
2) Tesfaye S, Selvarajah D. Advances in the epidemiology, pathogenesis and management of diabetic peripheral neuropathy. Diabetes Metab Res Rev 2012; 28 Suppl 1: 8-14.
3) Lotfy M, Adeghate J, Kalasz H, Singh J, Adeghate E. Chronic complications of diabetes mellitus: a mini review. Curr Diabetes Rev 2017; 13: 3-10.
4) Tesfaye S, Selvarajah D, Gandhi R, Greig M, Shillo P, Fang F, Wilkinson ID. Diabetic peripheral neuropathy may not be as its name suggests: evidence from magnetic resonance imaging. Pain 2016; 157 Suppl 1: S72-S80.

5) Tesfaye S, Boulton AJ, Dyck PJ, Freeman R, Horowitz M, Kempler P, Lauria G, Malik RA, Spallone V, Vinik A, Bernardi L, Valensi P. Diabetic neuropathies: update on definitions, diagnostic criteria, estimation of severity, and treatments. Diabetes Care 2010; 33: 2285-2293.
6) Dyck PJ, Kratz KM, Karnes JL, Litchy WJ, Klein R, Pach JM, Wilson DM, O'Brien PC, Melton LR, Service FJ. The prevalence by staged severity of various types of diabetic neuropathy, retinopathy, and nephropathy in a population-based cohort: the Rochester Diabetic Neuropathy Study. Neurology 1993; 43: 817-824.
7) Sadosky A, McDermott AM, Brandenburg NA, Strauss M. A review of the epidemiology of painful diabetic peripheral neuropathy, postherpetic neuralgia, and less commonly studied neuropathic pain conditions. Pain Pract 2008; 8: 45-56.
8) Bhatheja K, Field J. Schwann cells: origins and role in axonal maintenance and regeneration. Int J Biochem Cell Biol 2006; 38: 1995-1999.
9) Goncalves NP, Vaegter CB, Andersen H, Ostergaard L, Calcutt NA, Jensen TS. Schwann cell interactions with axons and microvessels in diabetic neuropathy. Nat Rev Neurol 2017; 13: 135-147.
10) Jaffey PB, Gelman BB. Increased vulnerability to demyelination in streptozotocin diabetic rats. J Comp Neurol 1996; 373: 55-61.
11) Pittenger GL, Liu D, Vinik AI. The toxic effects of serum from patients with type 1 diabetes mellitus on mouse neuroblastoma cells: a new mechanism for development of diabetic autonomic neuropathy. Diabet Med 1993; 10: 925-932.
12) Farag YM, Gaballa MR. Diabesity: an overview of a rising epidemic. Nephrol Dial Transplant 2011; 26: 28-35.
13) Wiggin TD, Sullivan KA, Pop-Busui R, Amato A, Sima AA, Feldman EL. Elevated triglycerides correlate with progression of diabetic neuropathy. Diabetes 2009; 58: 1634-1640.
14) Voss U, Sand E, Olde B, Ekblad E. Enteric neuropathy can be induced by high fat diet in vivo and palmitic acid exposure in vitro. Plos One 2013; 8: e81413.
15) El-Assaad W, Buteau J, Peyot ML, Nolan C, Roduit R, Hardy S, Joly E, Dbaibo G, Rosenberg L, Prentki M. Saturated fatty acids synergize with elevated glucose to cause pancreatic beta-cell death. Endocrinology 2003; 144: 4154-4163.
16) Rho MC, Ah LK, Mi KS, Sik LC, Jeong JM, Kook KY, Sun LH, Hyun CY, Yong RB, Kim K. Sensitization of vascular smooth muscle cell to TNF-alpha-mediated death in the presence of palmitate. Toxicol Appl Pharmacol 2007; 220: 311-319.
17) Wei Y, Wang D, Topczewski F, Pagliassotti MJ. Saturated fatty acids induce endoplasmic reticulum stress and apoptosis independently of ceramide in liver cells. Am J Physiol Endocrinol Metab 2006; 291: E275-E281.
18) Malecki A, Garrido R, Mattson MP, Hennig B, Toborek M. 4-Hydroxynonenal induces oxidative stress and death of cultured spinal cord neurons. J Neurochem 2000; 74: 2278-2287.
19) Conti AC, Raghupathi R, Trojanowski JQ, McIntosh TK. Experimental brain injury induces regionally distinct apoptosis during the acute and delayed post-traumatic period. J Neurosci 1998; 18: 5663-5672.
20) Farmer KL, Li C, Dobrowsky RT. Diabetic peripheral neuropathy: should a chaperone accompany our therapeutic approach? Pharmacol Rev 2012; 64: 880-900.
21) O'Brien PD, Hinder LM, Sakowski SA, Feldman EL. ER stress in diabetic peripheral neuropathy: a new therapeutic target. Antioxid Redox Signal 2014; 21: 621-633.
22) Lupachyk S, Watcho P, Obrosov AA, Stavniichuk R, Obrosova IG. Endoplasmic reticulum stress contributes to prediabetic peripheral neuropathy. Exp Neurol 2013; 247: 342-348.
23) Schroder M, Kaufman RJ. The mammalian unfolded protein response. Annu Rev Biochem 2005; 74: 739-789.
24) Sano R, Reed JC. ER stress-induced cell death mechanisms. Biochim Biophys Acta 2013; 1833: 3460-3470.
25) Lupachyk S, Watcho P, Stavniichuk R, Shevalye H, Obrosova IG. Endoplasmic reticulum stress plays a key role in the pathogenesis of diabetic peripheral neuropathy. Diabetes 2013; 62: 944-952.
26) Fiennes AG, Walton J, Winterbourne D, McGlashan D, Hermon-Taylor J. Quantitative correlation of neutral red dye uptake with cell number in human cancer cell cultures. Cell Biol Int Rep 1987; 11: 373-378.
27) Bonaventura P, Lamboux A, Albarede F, Miossec P. Regulatory effects of zinc on cadmium-induced cytotoxicity in chronic inflammation. Plos One 2017; 12: e180879.
28) Attarde SS, Pandit SV. Cytotoxic activity of NN-32 toxin from Indian spectacled cobra venom on human breast cancer cell lines. BMC Complement Altern Med 2017; 17: 503.
29) Porter AG, Janicke RU. Emerging roles of caspase-3 in apoptosis. Cell Death Differ 1999; 6: 99-104.
30) Imada M, Sueoka N. Clonal sublines of rat neurotumor RT4 and cell differentiation. I. Isolation and characterization of cell lines and cell type conversion. Dev Biol 1978; 66: 97-108.
31) Kimura H, Fischer WH, Schubert D. Structure, expression and function of a schwannoma-derived growth factor. Nature 1990; 348: 257-260.
32) Ridley AJ, Paterson HF, Noble M, Land H. Ras-mediated cell cycle arrest is altered by nuclear oncogenes to induce Schwann cell transformation. EMBO J 1988; 7: 1635-1645.
33) Badache A, De Vries GH. Neurofibrosarcoma-derived Schwann cells overexpress platelet-derived growth factor (PDGF) receptors and are induced to proliferate by PDGF BB. J Cell Physiol 1998; 177: 334-342.
34) Toda K, Small JA, Goda S, Quarles RH. Biochemical and cellular properties of three immortalized Schwann cell lines expressing different levels of the myelin-associated glycoprotein. J Neurochem 1994; 63: 1646-1657.
35) Hai M, Muja N, DeVries GH, Quarles RH, Patel PI. Comparative analysis of Schwann cell lines

as model systems for myelin gene transcription studies. J Neurosci Res 2002; 69: 497-508.
36) Rutkowski DT, Kaufman RJ. A trip to the ER: coping with stress. Trends Cell Biol 2004; 14: 20-28.
37) Kaufman RJ. Stress signaling from the lumen of the endoplasmic reticulum: coordination of gene transcriptional and translational controls. Genes Dev 1999; 13: 1211-1233.
38) Ron D. Translational control in the endoplasmic reticulum stress response. J Clin Invest 2002; 110: 1383-1388.
39) Harding HP, Calfon M, Urano F, Novoa I, Ron D. Transcriptional and translational control in the Mammalian unfolded protein response. Annu Rev Cell Dev Biol 2002; 18: 575-599.
40) Kozutsumi Y, Segal M, Normington K, Gething MJ, Sambrook J. The presence of malfolded proteins in the endoplasmic reticulum signals the induction of glucose-regulated proteins. Nature 1988; 332: 462-464.
41) Rao RV, Bredesen DE. Misfolded proteins, endoplasmic reticulum stress and neurodegeneration. Curr Opin Cell Biol 2004; 16: 653-662.
42) Ferri KF, Kroemer G. Organelle-specific initiation of cell death pathways. Nat Cell Biol 2001; 3: E255-E263.
43) Malhotra JD, Kaufman RJ. The endoplasmic reticulum and the unfolded protein response. Semin Cell Dev Biol 2007; 18: 716-731.
44) Yasuda H, Terada M, Maeda K, Kogawa S, Sanada M, Haneda M, Kashiwagi A, Kikkawa R. Diabetic neuropathy and nerve regeneration. Prog Neurobiol 2003; 69: 229-285.
45) Dey A, Kessova IG, Cederbaum AI. Decreased protein and mRNA expression of ER stress proteins GRP78 and GRP94 in HepG2 cells over-expressing CYP2E1. Arch Biochem Biophys 2006; 447: 155-166.
46) Jamora C, Dennert G, Lee AS. Inhibition of tumor progression by suppression of stress protein GRP78/BiP induction in fibrosarcoma B/C10ME. Proc Natl Acad Sci U S A 1996; 93: 7690-7694.
47) Zhang J, Jiang Y, Jia Z, Li Q, Gong W, Wang L, Wei D, Yao J, Fang S, Xie K. Association of elevated GRP78 expression with increased lymph node metastasis and poor prognosis in patients with gastric cancer. Clin Exp Metastasis 2006; 23: 401-410.
48) Scheuner D, Song B, McEwen E, Liu C, Laybutt R, Gillespie P, Saunders T, Bonner-Weir S, Kaufman RJ. Translational control is required for the unfolded protein response and in vivo glucose homeostasis. Mol Cell 2001; 7: 1165-1176.
49) Harding HP, Novoa I, Zhang Y, Zeng H, Wek R, Schapira M, Ron D. Regulated translation initiation controls stress-induced gene expression in mammalian cells. Mol Cell 2000; 6: 1099-1108.
50) Eizirik DL, Cardozo AK, Cnop M. The role for endoplasmic reticulum stress in diabetes mellitus. Endocr Rev 2008; 29: 42-61.
51) Oyadomari S, Mori M. Roles of CHOP/GADD153 in endoplasmic reticulum stress. Cell Death Differ 2004; 11: 381-389.
52) Schumacher M, Jung-Testas I, Robel P, Baulieu EE. Insulin-like growth factor I: a mitogen for rat Schwann cells in the presence of elevated levels of cyclic AMP. Glia 1993; 8: 232-240.
53) Khodabandehloo H, Gorgani-Firuzjaee S, Panahi G, Meshkani R. Molecular and cellular mechanisms linking inflammation to insulin resistance and beta-cell dysfunction. Transl Res 2016; 167: 228-256.
54) Jin HY, Lee KA, Park TS. The impact of glycemic variability on diabetic peripheral neuropathy. Endocrine 2016; 53: 643-648.
55) Quagliaro L, Piconi L, Assaloni R, Martinelli L, Motz E, Ceriello A. Intermittent high glucose enhances apoptosis related to oxidative stress in human umbilical vein endothelial cells: the role of protein kinase C and NAD(P)H-oxidase activation. Diabetes 2003; 52: 2795-2804.
56) Kim MJ, Jung HS, Hwang-Bo Y, Cho SW, Jang HC, Kim SY, Park KS. Evaluation of 1,5-anhydroglucitol as a marker for glycemic variability in patients with type 2 diabetes mellitus. Acta Diabetol 2013; 50: 505-510.
57) Delaney CL, Russell JW, Cheng HL, Feldman EL. Insulin-like growth factor-I and over-expression of Bcl-xL prevent glucose-mediated apoptosis in Schwann cells. J Neuropathol Exp Neurol 2001; 60: 147-160.
58) Min S, Jian-bo L, Hong-man Z, Ling-fei Y, Min X, Jia-wei C. Neuritin is expressed in Schwann cells and down-regulated in apoptotic Schwann cells under hyperglycemia. Nutr Neurosci 2012; 15: 264-270.